

Enhancement of Chiral-Induced Spin Selectivity via Circularly Polarized Light

Wei Liu and Jingqi Chen

Department of Chemistry, School of Science, Westlake University, Hangzhou 310024 Zhejiang, China and
Institute of Natural Sciences, Westlake Institute for Advanced Study, Hangzhou 310024 Zhejiang, China

Wenjie Dou*

Department of Chemistry, School of Science, Westlake University, Hangzhou 310024 Zhejiang, China
Department of Physics, School of Science, Westlake University, Hangzhou 310024 Zhejiang, China and
Institute of Natural Sciences, Westlake Institute for Advanced Study, Hangzhou 310024 Zhejiang, China

(Dated: February 5, 2024)

The notion of chiral-induced spin selectivity (CISS) has attracted intensive research interest recently. However, the practical applications of the CISS effects face challenges due to relatively low spin polarization. In this Letter, we propose a non-perturbative theory illustrating how circularly polarized (CP) light enhances CISS effects through strong light-matter interactions. We introduce a Floquet electronic friction model to study the nonadiabatic dynamics and spin transport through a chiral molecule in a molecule junction subjected to external driving. Our results show that the interplay of the nonadiabatic effects and light-matter interactions can significantly ($> 90\%$) enhance electron spin polarization under CP light. Our predictions can be very useful in experiments for using CP light to control spin current in chiral molecular junctions.

Introduction.—Chirality characterizes parity-symmetry breaking where a molecule cannot be superposed on its mirror image in chemistry and biology [1–3]. Chiral organics have recently been reported to exhibit a topological feature [4], in which the electronic orbital and momentum are locked together, to rationalize the intriguing spin selectivity in DNA-type molecules [5, 6], known as CISS [7]. The CISS effects were initially reported in 1999 by Naaman and collaborators[7]. Since then, a number of additional experimental [8–23] and theoretical [4, 24–64] studies have been conducted. A future industrial applications of CISS is spin-based chip design, which should enable electronic devices to reach atomic scale [65, 66]. Although we can observe up to 85% spin polarization in experiments using the contact magnetic atomic force microscope (AFM) setup [67], spin selection occurs prior to electron passage through the chiral molecule, and this initial spin selection is primarily due to the strong SOC of the metal substrate [61]. The SOC alone induced by electron motion within chiral molecules [54] is too small to give rise to the observed spin polarization [68]. How to enhance CISS has attracted extensive research.

Recent studies indicate that electron-vibration coupling enhances the CISS effect, leading to an increase in the spin polarization in double-helix DNA [62]. When considering the coupling between atomic nuclei and electron spins, calculations reveal strong spin selectivity near the conical intersection, even when the SOC is small, with spin selectivity reaching up to 100% [63]. In the presence of a non-zero current, Berry curvature can induce nuclear spin separation and electron spin polarization [64]. However, the universal theory on how to enhance CISS is still lacking.

In physics, chirality usually refers to the spin–momentum locking of particles such as Weyl fermions [69, 70] and CP light. Chiral enantiomers exhibit opposite chiroptical activity when coupling to light [71]. Due to the dissymmetric

interaction between CP light and chiral molecules, there is a selectivity in absorption or emission of left-handed versus right-handed CP light for chiral molecular systems [72, 73]. Therefore, inspired by the close connection between chiral molecules and light-matter interactions, we sought to explore whether CP light could enhance the CISS, contributing to the ongoing advancements in spintronics [5, 74].

In this Letter, we present a non-perturbative theory to illustrate how circularly polarized (CP) light enhances CISS through strong light-matter interactions. Our results indicate that when chiral molecules interact with CP light, there is a significant ($> 90\%$) enhancement of electron spin polarization. The prediction from our newly developed theory highlights the effects of using CP light to control spin current in a chiral molecular junction, which can be potentially verified in CISS experiments.

General Hamiltonian.—As shown in the schematic diagram [Fig. 1 (a)], we start from a minimal model for CISS with two spatial orbitals and spin-orbit couplings between them [8, 64]. These orbitals couple to left and right leads whose voltages are μ_L and μ_R , respectively. In addition, the Hamiltonian depends on two nuclear degrees of freedom (x and y are considered, uniformly represented as \mathbf{R}). The total model Hamiltonian \hat{H}_{tot} consists of the kinetic energy and another three parts: the system Hamiltonian \hat{H}_s , the bath Hamiltonian \hat{H}_b composed of left and right leads, and the system-bath coupling Hamiltonian \hat{H}_{sb} ,

$$\hat{H}_{\text{tot}} = \frac{\hat{p}^2}{2M} + \hat{H}_s + \hat{H}_b + \hat{H}_{\text{sb}}, \quad (1)$$

$$\hat{H}_s = \sum_{ij} [h_s]_{ij}(\mathbf{R}, t) \hat{d}_i^\dagger \hat{d}_j + U(\mathbf{R}), \quad (2)$$

$$\hat{H}_b = \sum_{k\zeta} \epsilon_{k\zeta} \hat{c}_{k\zeta}^\dagger \hat{c}_{k\zeta}, \quad (3)$$

$$\hat{H}_{\text{sb}} = \sum_{\zeta k, i} V_{\zeta k, i} (\hat{c}_{k\zeta}^\dagger \hat{d}_i + \hat{d}_i^\dagger \hat{c}_{k\zeta}). \quad (4)$$

In system Hamiltonian (\hat{H}_s), the operators \hat{d}_i^\dagger and \hat{d}_i denote create and annihilate an electron in the i -th spin orbital of the subsystem respectively. $U(\mathbf{R})$ represents the electrostatic potential between nuclei. As for the Hamiltonian (\hat{H}_b), the op-

* douwenjie@westlake.edu.cn

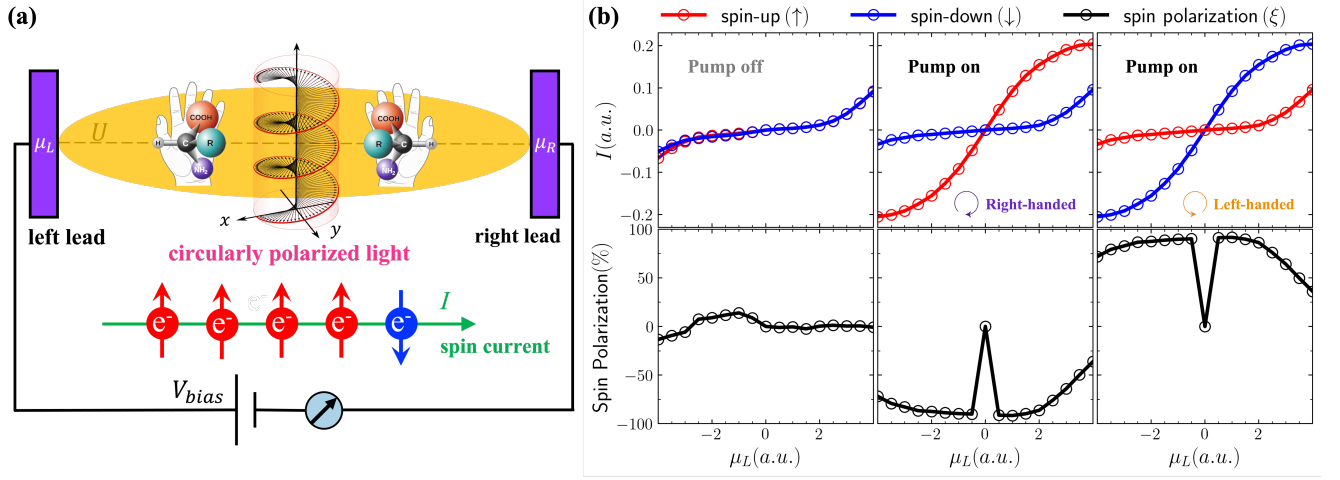


FIG. 1. (a) A schematic picture of our chiral molecular junction model interacted with circularly polarized light. μ_L and μ_R are chemical potentials of the left and right leads, and the source-drain voltage $V_{sd} = \mu_L - \mu_R$ controls the voltage bias V_{bias} . (b) Steady-state spin current $I^{\uparrow/\downarrow}$ in Eq. 13 and spin polarization ξ in Eq. 18 for h_s (pump off) in Eq. 7, $h_s^{[R]}$ (pump on and right-handed) in Eq. 5 and $h_s^{[L]}$ (pump on and left-handed) in Eq. 6. For spin-up and spin-down electrons, we calculate the average spin current using 10^4 nuclear motion trajectories with random force δF_{μ}^F , respectively. Parameters: $\Delta = 3$, $A = B = 1$, $\Omega = 1$, $kT = 0.5$, $\lambda_x = 0$, $\lambda_y = 0.8$, $\tilde{\Gamma} = 1$, $\mu_L = -\mu_R$ and Floquet level $N = 5$.

erators $\hat{c}_{k\zeta}^\dagger$ and $\hat{c}_{k\zeta}$ create and annihilate electrons in the k -th spin orbital of the lead ζ , where the energy of the orbital is denoted by $\epsilon_{k\zeta}$. Lastly, in the interaction Hamiltonian (\hat{H}_{sb}), the tunneling element $V_{\zeta k,i}$ indicates the interaction between subsystem spin orbital i and lead spin orbital $k\zeta$. In Eq. 4, the Condon approximation has been utilized, implying that $V_{\zeta k,i}$ is independent of \mathbf{R} .

For the system Hamiltonian, we consider chiral molecules interacting with a CP light beam, which involves periodic driving from light-matter interactions. For right-handed/clockwise CP light, the system Hamiltonian $h_s^{[R]}$ writes

$$h_s^{[R]}(\mathbf{R}, t) = \begin{bmatrix} x + \Delta & Ax \cos(\Omega t) - iBy \sin(\Omega t) \\ Ax \cos(\Omega t) + iBy \sin(\Omega t) & -x - \Delta \end{bmatrix}. \quad (5)$$

While for left-handed/counterclockwise CP light, the system Hamiltonian $h_s^{[L]}$ writes

$$h_s^{[L]}(\mathbf{R}, t) = \begin{bmatrix} x + \Delta & Ax \cos(\Omega t) + iBy \sin(\Omega t) \\ Ax \cos(\Omega t) - iBy \sin(\Omega t) & -x - \Delta \end{bmatrix}. \quad (6)$$

Floquet Nonadiabatic Dynamics.—We adapt our newly developed Floquet electronic friction model to study nonadiabatic spin transport dynamics [77, 78]. In particular, all electronic DoFs (including spin-orbit couplings) as well as periodic driving are being incorporated into frictional force and random force on nuclear motion. As a result, one can simply run Langevin equation of motion for the nuclei, which is given

Finally, for no polarized light, the system Hamiltonian h_s writes

$$h_s(\mathbf{R}, t) = \begin{bmatrix} x + \Delta & Ax - iBy \\ Ax + iBy & -x - \Delta \end{bmatrix}. \quad (7)$$

Here, Δ represents the energy gap between two spatial orbitals, parameter A denotes the shifts of diabatic PES and B denotes the strength of spin-orbit couplings. Moreover, Ω denotes the frequency of the periodic driving.

The shifted parabola model is extensively employed to simulate electron transfer and excitation energy transfer processes [75]. Note that Eq. 5, Eq. 6 and Eq. 7 are all effective Hamiltonians, where positive B represents spin-up state and negative B represents spin-down state.

As commonly used in literature [76], the bare potential $U(\mathbf{R})$ is set to be a two dimensional parabolas:

$$U(\mathbf{R}) = \frac{1}{2}(x - \lambda_x x)^2 + \frac{1}{2}(y - \lambda_y y)^2. \quad (8)$$

Even though the scalar potential $U(\mathbf{R})$ does not couple to spin state directly, the linear terms λ_x and λ_y in $U(\mathbf{R})$ can change the spin current and spin polarization dramatically. At this point, we have introduced our model for spin transport in a chiral molecule with optical control.

by

$$M_\mu \ddot{\mathbf{R}}_\mu = F_\mu^F - \sum_\nu \gamma_{\mu\nu}^F \dot{\mathbf{R}}_\nu + \delta F_\mu^F. \quad (9)$$

Here, F_μ^F , $\gamma_{\mu\nu}^F$, and δF_μ^F are mean force, friction tensor, and random force respectively. We use the superscript F to denote their Floquet counterparts. To evaluate F_μ^F , $\gamma_{\mu\nu}^F$, and δF_μ^F , we

need to represent $h_s^{[R]}$ and $h_s^{[L]}$ in Floquet levels. Here, we provide an explicit formula for each block of the extensive matrix, which is in the Fourier space:

$$h_s^F = \sum_{n=-N}^N [h_s^{[R]/[L]}]^{(n)} \hat{L}_n + \hat{N} \otimes \hat{I}_n \hbar \omega, \quad (10)$$

$$[h_s^{[R]/[L]}]^{(n)} = \frac{1}{T} \int_0^T h_s^{[R]/[L]}(\mathbf{R}, t) e^{-in\Omega t} dt, \quad (11)$$

where \hat{N} is the number operator, \hat{I}_n is the identity matrix for the n -th order and T is the period, equal to $2\pi/\Omega$. \hat{L}_n is the n -th ladder operator which turns the vector-like Fourier expansion into a matrix-like representation. Specifically, Eq. 10 represents the decomposition of $h_s^{[R]/[L]}(\mathbf{R}, t)$ into different energy components rotating at different frequencies in the Fourier space. The term $[h_s^{[R]/[L]}]^{(n)}$ denotes the decomposition of $h_s^{[R]/[L]}(\mathbf{R}, t)$ at the frequency of $n\Omega$. The first term of Eq. 10 is the weighted sum of each Floquet potential, while the second term is the tensor product of \hat{N} and \hat{I}_n . This term can be added to the Hamiltonian because \hat{N} commutes with the Hamiltonian. Eq. 10 allows us to understand the time evolution of the system at different rotating frequencies, and further investigate the physical properties of the system.

The explicit form of the frictional force and random force are computed directly in terms of Green's functions. The frictional force is given by

$$\gamma_{\mu\nu}^F = -\frac{\hbar}{2\pi(2N+1)} \int_{-\infty}^{+\infty} d\varepsilon \text{Tr} \{ \partial_\mu h_s^F \partial_\varepsilon G_r^F \partial_\nu h_s^F G_{<}^F \} + \text{H.c.} \quad (12)$$

Please refer to Supplemental Material (SM) A for details.

Spin Current.—The spin current $I^{\uparrow/\downarrow}$ is obtained by averaging over the nuclear DOFs with respect to local current [64]:

$$I^{\uparrow/\downarrow} = \int d\mathbf{R} d\mathbf{P} I_{\text{loc}}^F(\mathbf{R}) \rho^{\uparrow/\downarrow}(\mathbf{R}, \mathbf{P}). \quad (13)$$

The local current I_{loc}^F flowing from the left lead through the molecule to the right lead can be evaluated by the Landauer formula [79, 80],

$$I_{\text{loc}}^F = \frac{e}{2\pi\hbar(2N+1)} \int_{-\infty}^{+\infty} d\varepsilon \text{Tr} \{ T^F(\varepsilon) [f_L^F(\varepsilon) - f_R^F(\varepsilon)] \}. \quad (14)$$

In the above equation, $f_L^F(\varepsilon)$ and $f_R^F(\varepsilon)$ represent the Floquet Fermi-Dirac distribution functions that correspond to the left and right leads, respectively. Additionally, $T^F(\varepsilon)$ denotes the Floquet transmission probability, which can be deconstructed using the Green's functions.

$$T^F(\varepsilon) = \Gamma_L^F G_r^F(\varepsilon) \Gamma_R^F G_a^F(\varepsilon), \quad (15)$$

where

$$\Gamma_L^F = \Gamma_L \otimes \hat{I}_n, \quad \Gamma_R^F = \Gamma_R \otimes \hat{I}_n. \quad (16)$$

In this project, we examine the distinct interaction between a molecule and two leads where solely orbital 1 ($x + \Delta$) couples to the left lead and only orbital 2 ($-x - \Delta$) couples to the right lead. This arrangement is demonstrated in the subsequent definition of the Γ matrices:

$$\Gamma_L = \begin{pmatrix} \tilde{\Gamma} & 0 \\ 0 & 0 \end{pmatrix}, \quad \Gamma_R = \begin{pmatrix} 0 & 0 \\ 0 & \tilde{\Gamma} \end{pmatrix}. \quad (17)$$

Finally, we define spin polarization ξ as follows,

$$\xi = \frac{I^\downarrow - I^\uparrow}{I^\downarrow + I^\uparrow} \times 100\%. \quad (18)$$

Here, $I^{\uparrow/\downarrow}$ denotes spin-up or spin-down current. See SM B for details of computing $I^{\uparrow/\downarrow}$.

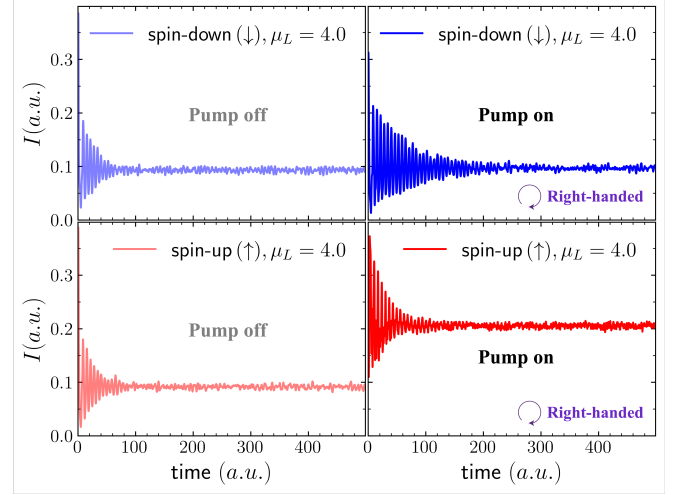


FIG. 2. Dynamics of spin current $I^{\uparrow/\downarrow}$ in Eq. 13 for h_s (pump off) in Eq. 7 and $h_s^{[R]}$ (pump on and right-handed) in Eq. 5 when $\mu_L = 4.0$ in Fig. 1 (b). All parameters are identical with Fig. 1 (b).

Spin Polarization Enhanced by CP Light.—We present the impact of CP light on enhancing spin polarization. In Fig. 1 (b), we illustrate the steady-state spin current and spin polarization for $\Delta = 3$ with $\mu_L = -\mu_R$.

In the left panel (pump off) of Fig. 1 (b), we plot the spin polarization/spin current without light-matter interactions (using h_s in Eq. 7). Without voltage bias, there is no spin polarization being observed. This finding agrees with experiments [64, 67]. When $-4 \leq \mu_L < 0$, CISS-induced spin polarization consistently remains below 25%, whereas for $0 < \mu_L \leq 4$, the spin polarization induced by CISS nearly diminishes. Notably, in the middle panel (pump on, right-handed) and right panel (pump on, left-handed) of Fig. 1 (b), activating right-handed ($h_s^{[R]}$) or left-handed ($h_s^{[L]}$) CP light results in high spin polarization ($|\xi| \approx 91\%$) at a small voltage bias ($\mu_L = \pm 0.5$). This spin polarization gradually diminishes as $|\mu_L|$ increases, consistently remaining above 25% within the range of $0 < |\mu_L| \leq 4$. The symmetric distribution of spin polarization caused by right-handed and left-handed CP light with respect to 0% is consistent with experiments [8]. Therefore, for simplicity, we only present the results of the right-hand CP light in Fig. 2 and Fig. 3. Note that the presence of

$\Delta = 3$ results in an asymmetric energy distribution for the two spatial orbitals. Therefore, the spin polarization for $\mu_L > 0$ decreases more rapidly compared to $\mu_L < 0$. Within the current range of results, it is evident that the decline in spin polarization persists with the increasing magnitude of $|\mu_L|$. Hence, we recommend employing a small V_{bias} for researchers aiming to observe conspicuous spin polarization in experiments.

In Fig. 2, we plot the dynamics of spin current with the comparison between no light (pump off) and right-handed CP light (pump on) when $\mu_L = 4.0$ in Fig. 1 (b). Spin current fluctuations arise from random forces and progressively diminish with an increasing number of trajectories, set at 10^4 for each spin state in this calculation. For spin-down electrons, CP light does not result in a significant enhancement of the steady-state current value; however, the time required to reach the steady state considerably prolongs, as illustrated in the upper panel of Fig. 2. In contrast, for spin-up electrons, the activation of CP light enhances both the steady-state value and the relaxation time of the spin current, as depicted in the lower panel of Fig. 2. This observation suggests that in this system, CP light introduces additional oscillations, and right-handed CP light specifically exhibits a more pronounced selectivity toward spin-up electrons.

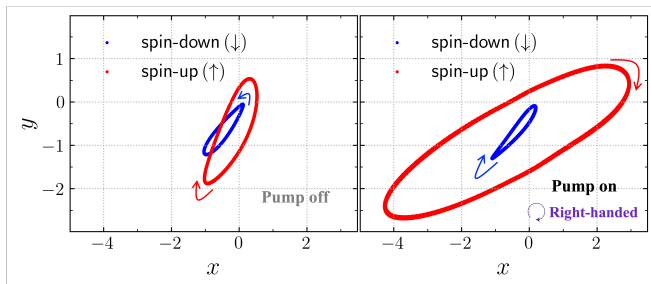


FIG. 3. Nuclear distribution $\rho^{\uparrow/\downarrow}$ ($300 \leq \text{time} \leq 2000$, $\Delta t = 0.05$) in Eq. 13 for h_s (pump off) in Eq. 7 and $h_s^{\text{[R]}}$ (pump on and right-handed) in Eq. 5 when $\mu_L = 4.0$ without the random force δF_μ^{F} from the Langevin dynamics to obtain the steady state distribution. All parameters are identical with Fig. 2.

In Fig. 3, we illustrate the nuclear distribution at $\mu_L = 4.0$ without the random force from Langevin dynamics, allowing us to obtain the steady-state distribution [81]. The distinct steady states observed in nuclei with spin-up and spin-down electrons, as depicted in Fig. 3, can be ascribed to the influence of the Lorentz-like force associated with the anti-symmetric friction tensor γ_{xy}^{A} [77]. When pump off, the steady state of nuclear motion exhibits counterclockwise rotation for spin-down electrons and clockwise rotation for spin-up electrons, as illustrated in Fig.3 (pump off). At this stage, the

difference in the distribution range between spin-up and spin-down states is minimal, as reflected in the spin current, where the distinction remains inconspicuous (Fig.2, pump off). Notably, upon the activation of CP light, the contrast in nuclear steady-state distribution between spin-up and spin-down electrons undergoes a significant amplification, as illustrated in Fig. 3 (pump on). This result corresponds with the marked rise in spin polarization depicted in Fig. 1 (b) [$\mu_L = 4.0$ for pump off and on (right-handed)]. The introduction of CP light emerges as a crucial factor in enhancing the distinctions in nuclear motion and spin polarization between spin-up and spin-down electronic states.

These findings highlight the critical role of the CP light in influencing the steady states of nuclear motion and, consequently, spin polarization in electronic systems. In addition to the specific cases discussed here, our results have broader implications for the fields of spintronics and optoelectronics. The ability to manipulate spin polarization through light-matter interactions opens up the possibilities for developing spin-based devices with tunable properties. Furthermore, the understanding of the underlying mechanisms, such as the influence of CP light, provides guidance for spin control and manipulation in designing novel materials and structures.

Conclusions.—In conclusion, our investigation into the influence of CP light on spin polarization in electronic systems has yielded valuable insights. We have demonstrated that CP light can exert a profound enhancement ($> 90\%$) on spin polarization. In particular, light-matter interactions introduce Lorentz-like force that changes the nuclear dynamics dramatically for different spin states. As a result, even small spin-orbit couplings (SOC) can introduce large spin selectivity. We find that the interplay of the light-matter interactions and SOC can enhance the spin polarization in quantum transport.

These findings not only advance our fundamental understanding of spin dynamics in optoelectronic systems but also open up exciting opportunities for practical applications in the realm of spintronics. The ability to control and manipulate spin polarization through light-matter interactions holds great promise for the development of novel technologies, including spin-based quantum computing and information storage.

As we peer into the future, several promising avenues for further research emerge. In the realm of electronic structure theory, there is an urgent need for high-precision calculations of excited-state electronic spin states in large systems, surpassing the capabilities of traditional Density Functional Theory (DFT). Accurately modeling spin-orbit coupling (SOC) as well as derivative couplings is equally crucial. These works are on-going.

This material is based upon work supported by National Natural Science Foundation of China (NSFC No. 22361142829). W.L. acknowledges support from the high-performance computing center of Westlake University.

-
- [1] M. Quack, Structure and dynamics of chiral molecules, *Angewandte Chemie International Edition in English* **28**, 571 (1989).
 [2] J. S. Siegel, Homochiral imperative of molecular evolution,

- Chirality: The Pharmacological, Biological, and Chemical Consequences of Molecular Asymmetry **10**, 24 (1998).
 [3] L. D. Barron, Symmetry and chirality: where physics shakes

- hands with chemistry and biology, *Israel Journal of Chemistry* **61**, 517 (2021).
- [4] Y. Liu, J. Xiao, J. Koo, and B. Yan, Chirality-driven topological electronic structure of dna-like materials, *Nature materials* **20**, 638 (2021).
- [5] R. Naaman, Y. Paltiel, and D. H. Waldeck, Chiral molecules and the electron spin, *Nature Reviews Chemistry* **3**, 250 (2019).
- [6] F. Evers, A. Aharony, N. Bar-Gill, O. Entin-Wohlman, P. Hedegård, O. Hod, P. Jelinek, G. Kamieniarz, M. Lemeshko, K. Michaeli, *et al.*, Theory of chirality induced spin selectivity: Progress and challenges, *Advanced Materials* **34**, 2106629 (2022).
- [7] K. Ray, S. Ananthavel, D. Waldeck, and R. Naaman, Asymmetric scattering of polarized electrons by organized organic films of chiral molecules, *Science* **283**, 814 (1999).
- [8] B. Göhler, V. Hamelbeck, T. Markus, M. Kettner, G. Hanne, Z. Vager, R. Naaman, and H. Zacharias, Spin selectivity in electron transmission through self-assembled monolayers of double-stranded dna, *Science* **331**, 894 (2011).
- [9] Z. Xie, T. Z. Markus, S. R. Cohen, Z. Vager, R. Gutierrez, and R. Naaman, Spin specific electron conduction through dna oligomers, *Nano letters* **11**, 4652 (2011).
- [10] O. Ben Dor, N. Morali, S. Yochelis, L. T. Baczewski, and Y. Paltiel, Local light-induced magnetization using nanodots and chiral molecules, *Nano letters* **14**, 6042 (2014).
- [11] V. Kiran, S. P. Mathew, S. R. Cohen, I. Hernández Delgado, J. Lacour, and R. Naaman, Helicenes—a new class of organic spin filter, *Advanced Materials* **28**, 1957 (2016).
- [12] M. Eckshtain-Levi, E. Capua, S. Refaely-Abramson, S. Sarkar, Y. Gavrilov, S. P. Mathew, Y. Paltiel, Y. Levy, L. Kronik, and R. Naaman, Cold denaturation induces inversion of dipole and spin transfer in chiral peptide monolayers, *Nature communications* **7**, 10744 (2016).
- [13] P. C. Mondal, P. Roy, D. Kim, E. E. Fullerton, H. Cohen, and R. Naaman, Photospintronics: magnetic field-controlled photoemission and light-controlled spin transport in hybrid chiral oligopeptide-nanoparticle structures, *Nano letters* **16**, 2806 (2016).
- [14] H. Alpern, E. Katzir, S. Yochelis, N. Katz, Y. Paltiel, and O. Millo, Unconventional superconductivity induced in nb films by adsorbed chiral molecules, *New Journal of Physics* **18**, 113048 (2016).
- [15] K. M. Alam and S. Pramanik, Spin filtering with poly-t wrapped single wall carbon nanotubes, *Nanoscale* **9**, 5155 (2017).
- [16] J. M. Abendroth, N. Nakatsuka, M. Ye, D. Kim, E. E. Fullerton, A. M. Andrews, and P. S. Weiss, Analyzing spin selectivity in dna-mediated charge transfer via fluorescence microscopy, *ACS nano* **11**, 7516 (2017).
- [17] A. Kumar, E. Capua, M. K. Kesharwani, J. M. Martin, E. Sitbon, D. H. Waldeck, and R. Naaman, Chirality-induced spin polarization places symmetry constraints on biomolecular interactions, *Proceedings of the National Academy of Sciences* **114**, 2474 (2017).
- [18] A. C. Aragonès, E. Medina, M. Ferrer-Huerta, N. Gimeno, M. Teixidó, J. L. Palma, N. Tao, J. M. Ugalde, E. Giral, I. Díez-Pérez, *et al.*, Measuring the spin-polarization power of a single chiral molecule, *small* **13**, 1602519 (2017).
- [19] V. Varade, T. Markus, K. Vankayala, N. Friedman, M. Sheves, D. H. Waldeck, and R. Naaman, Bacteriorhodopsin based non-magnetic spin filters for biomolecular spintronics, *Physical Chemistry Chemical Physics* **20**, 1091 (2018).
- [20] J. I. Santos, I. Rivilla, F. P. Cossio, J. M. Matxain, M. Grzelczak, S. K. Mazinani, J. M. Ugalde, and V. Mujica, Chirality-induced electron spin polarization and enantiospecific response in solid-state cross-polarization nuclear magnetic resonance, *ACS nano* **12**, 11426 (2018).
- [21] M. Gazzotti, S. Arnaboldi, S. Grecchi, R. Giovanardi, M. Cannio, L. Pasquali, A. Giacomino, O. Abollino, and C. Fontanesi, Spin-dependent electrochemistry: Enantio-selectivity driven by chiral-induced spin selectivity effect, *Electrochimica Acta* **286**, 271 (2018).
- [22] T. Shapira, H. Alpern, S. Yochelis, T.-K. Lee, C.-C. Kaun, Y. Paltiel, G. Koren, and O. Millo, Unconventional order parameter induced by helical chiral molecules adsorbed on a metal proximity coupled to a superconductor, *Physical Review B* **98**, 214513 (2018).
- [23] K. Ghosh, W. Zhang, F. Tassinari, Y. Mastai, O. Lidor-Shalev, R. Naaman, P. Mollers, D. Nurenberg, H. Zacharias, J. Wei, *et al.*, Controlling chemical selectivity in electrocatalysis with chiral cuo-coated electrodes, *The Journal of Physical Chemistry C* **123**, 3024 (2019).
- [24] M. Brandbyge, J.-L. Mozos, P. Ordejón, J. Taylor, and K. Stokbro, Density-functional method for nonequilibrium electron transport, *Physical Review B* **65**, 165401 (2002).
- [25] B. K. Nikolić and S. Souma, Decoherence of transported spin in multichannel spin-orbit-coupled spintronic devices: Scattering approach to spin-density matrix from the ballistic to the localized regime, *Physical Review B* **71**, 195328 (2005).
- [26] M. Paulsson, T. Frederiksen, H. Ueba, N. Lorente, and M. Brandbyge, Unified description of inelastic propensity rules for electron transport through nanoscale junctions, *Physical Review Letters* **100**, 226604 (2008).
- [27] S. Yeganeh, M. A. Ratner, E. Medina, and V. Mujica, Chiral electron transport: Scattering through helical potentials, *The Journal of chemical physics* **131** (2009).
- [28] D. A. Areshkin and B. K. Nikolić, Electron density and transport in top-gated graphene nanoribbon devices: First-principles green function algorithms for systems containing a large number of atoms, *Physical Review B* **81**, 155450 (2010).
- [29] A.-M. Guo and Q.-f. Sun, Spin-selective transport of electrons in dna double helix, *Physical review letters* **108**, 218102 (2012).
- [30] R. Gutierrez, E. Díaz, R. Naaman, and G. Cuniberti, Spin-selective transport through helical molecular systems, *Physical Review B* **85**, 081404 (2012).
- [31] A.-M. Guo and Q.-F. Sun, Spin-dependent electron transport in protein-like single-helical molecules, *Proceedings of the National Academy of Sciences* **111**, 11658 (2014).
- [32] H.-N. Wu, Y.-L. Zhu, X. Sun, and W.-J. Gong, Spin polarization and spin separation realized in the double-helical molecules, *Physica E: Low-dimensional Systems and Nanostructures* **74**, 156 (2015).
- [33] P.-H. Chang, T. Markussen, S. Smidstrup, K. Stokbro, and B. K. Nikolić, Nonequilibrium spin texture within a thin layer below the surface of current-carrying topological insulator Bi_2Se_3 : A first-principles quantum transport study, *Physical Review B* **92**, 201406 (2015).
- [34] E. Medina, L. A. González-Arraga, D. Finkelstein-Shapiro, B. Berche, and V. Mujica, Continuum model for chiral induced spin selectivity in helical molecules, *The Journal of chemical physics* **142** (2015).
- [35] J. M. Marmolejo-Tejada, K. Dolui, P. Lazic, P.-H. Chang, S. Smidstrup, D. Stradi, K. Stokbro, and B. K. Nikolic, Proximity band structure and spin textures on both sides of topological-insulator/ferromagnetic-metal interface and their charge transport probes, *Nano Letters* **17**, 5626 (2017).
- [36] K. Michaeli and R. Naaman, Origin of spin-dependent tunneling through chiral molecules, *The Journal of Physical Chemistry C* **123**, 17043 (2019).

- [37] S. Matityahu, Y. Utsumi, A. Aharony, O. Entin-Wohlman, and C. A. Balseiro, Spin-dependent transport through a chiral molecule in the presence of spin-orbit interaction and nonunitary effects, *Physical Review B* **93**, 075407 (2016).
- [38] S. Varela, V. Mujica, and E. Medina, Effective spin-orbit couplings in an analytical tight-binding model of dna: Spin filtering and chiral spin transport, *Physical Review B* **93**, 155436 (2016).
- [39] T.-R. Pan, A.-M. Guo, and Q.-F. Sun, Spin-polarized electron transport through helicene molecular junctions, *Physical Review B* **94**, 235448 (2016).
- [40] S. Matityahu, A. Aharony, O. Entin-Wohlman, and C. A. Balseiro, Spin filtering in all-electrical three-terminal interferometers, *Physical Review B* **95**, 085411 (2017).
- [41] T. Schmaltz, B. Gothe, A. Krause, S. Leitherer, H.-G. Steinrück, M. Thoss, T. Clark, and M. Halik, Effect of structure and disorder on the charge transport in defined self-assembled monolayers of organic semiconductors, *ACS nano* **11**, 8747 (2017).
- [42] E. Díaz, A. Contreras, J. Hernández, and F. Domínguez-Adame, Effective nonlinear model for electron transport in deformable helical molecules, *Physical Review E* **98**, 052221 (2018).
- [43] E. Díaz, F. Domínguez-Adame, R. Gutierrez, G. Cuniberti, and V. Mujica, Thermal decoherence and disorder effects on chiral-induced spin selectivity, *The Journal of Physical Chemistry Letters* **9**, 5753 (2018).
- [44] M. Palsgaard, T. Markussen, T. Gunst, M. Brandbyge, and K. Stokbro, Efficient first-principles calculation of phonon-assisted photocurrent in large-scale solar-cell devices, *Physical Review Applied* **10**, 014026 (2018).
- [45] M. Thoss and F. Evers, Perspective: Theory of quantum transport in molecular junctions, *The Journal of chemical physics* **148** (2018).
- [46] V. V. Maslyuk, R. Gutierrez, A. Dianat, V. Mujica, and G. Cuniberti, Enhanced magnetoresistance in chiral molecular junctions, *The journal of physical chemistry letters* **9**, 5453 (2018).
- [47] D. Nürenberg and H. Zacharias, Evaluation of spin-flip scattering in chirality-induced spin selectivity using the riccati equation, *Physical Chemistry Chemical Physics* **21**, 3761 (2019).
- [48] D. S. Kosov, Telegraph noise in markovian master equation for electron transport through molecular junctions, *The Journal of Chemical Physics* **148** (2018).
- [49] S. L. Rudge and D. S. Kosov, Distribution of residence times as a marker to distinguish different pathways for quantum transport, *Physical Review E* **94**, 042134 (2016).
- [50] N. Papior, N. Lorente, T. Frederiksen, A. García, and M. Brandbyge, Improvements on non-equilibrium and transport green function techniques: The next-generation transiesta, *Computer Physics Communications* **212**, 8 (2017).
- [51] X. Yang, C. H. van der Wal, and B. J. van Wees, Spin-dependent electron transmission model for chiral molecules in mesoscopic devices, *Physical Review B* **99**, 024418 (2019).
- [52] T. Holder, D. Kaplan, and B. Yan, Consequences of time-reversal-symmetry breaking in the light-matter interaction: Berry curvature, quantum metric, and diabatic motion, *Physical Review Research* **2**, 033100 (2020).
- [53] J. Bätge, Y. Ke, C. Kaspar, and M. Thoss, Nonequilibrium open quantum systems with multiple bosonic and fermionic environments: A hierarchical equations of motion approach, *Physical Review B* **103**, 235413 (2021).
- [54] Y. Wolf, Y. Liu, J. Xiao, N. Park, and B. Yan, Unusual spin polarization in the chirality-induced spin selectivity, *ACS nano* **16**, 18601 (2022).
- [55] T. D. Honeychurch and D. S. Kosov, Quantum transport in driven systems with vibrations: Floquet nonequilibrium green's functions and the self-consistent born approximation, *Physical Review B* **107**, 035410 (2023).
- [56] A. B. Lorentzen, M. Bouatou, C. Chacon, Y. J. Dappe, J. Lagoute, and M. Brandbyge, Quantum transport in large-scale patterned nitrogen-doped graphene, *Nanomaterials* **13**, 2556 (2023).
- [57] S. L. Rudge, Y. Ke, and M. Thoss, Current-induced forces in nanosystems: A hierarchical equations of motion approach, *Physical Review B* **107**, 115416 (2023).
- [58] Y. Adhikari, T. Liu, H. Wang, Z. Hua, H. Liu, E. Lochner, P. Schlottmann, B. Yan, J. Zhao, and P. Xiong, Interplay of structural chirality, electron spin and topological orbital in chiral molecular spin valves, *Nature Communications* **14**, 5163 (2023).
- [59] L. Wan, Y. Liu, M. J. Fuchter, and B. Yan, Anomalous circularly polarized light emission in organic light-emitting diodes caused by orbital-momentum locking, *Nature Photonics* **17**, 193 (2023).
- [60] J. E. Subotnik, Chiral molecules to transmit electron spin, *Science* **382**, 160 (2023).
- [61] J. Gersten, K. Kaasbjerg, and A. Nitzan, Induced spin filtering in electron transmission through chiral molecular layers adsorbed on metals with strong spin-orbit coupling, *The Journal of chemical physics* **139** (2013).
- [62] G.-F. Du, H.-H. Fu, and R. Wu, Vibration-enhanced spin-selective transport of electrons in the dna double helix, *Physical Review B* **102**, 035431 (2020).
- [63] Y. Wu and J. E. Subotnik, Electronic spin separation induced by nuclear motion near conical intersections, *Nature communications* **12**, 700 (2021).
- [64] H.-H. Teh, W. Dou, and J. E. Subotnik, Spin polarization through a molecular junction based on nuclear berry curvature effects, *Physical Review B* **106**, 184302 (2022).
- [65] J. Kim, A. Paul, P. A. Crowell, S. J. Koester, S. S. Sapatnekar, J.-P. Wang, and C. H. Kim, Spin-based computing: Device concepts, current status, and a case study on a high-performance microprocessor, *Proceedings of the IEEE* **103**, 106 (2014).
- [66] J. R. Brandt, F. Salerno, and M. J. Fuchter, The added value of small-molecule chirality in technological applications, *Nature Reviews Chemistry* **1**, 0045 (2017).
- [67] R. Naaman, Y. Paltiel, and D. H. Waldeck, Chiral molecules and the spin selectivity effect, *The journal of physical chemistry letters* **11**, 3660 (2020).
- [68] L. Zhang, Y. Hao, W. Qin, S. Xie, and F. Qu, Chiral-induced spin selectivity: A polaron transport model, *Physical Review B* **102**, 214303 (2020).
- [69] N. Armitage, E. Mele, and A. Vishwanath, Weyl and dirac semimetals in three-dimensional solids, *Reviews of Modern Physics* **90**, 015001 (2018).
- [70] B. Yan and C. Felser, Topological materials: Weyl semimetals, *Annual Review of Condensed Matter Physics* **8**, 337 (2017).
- [71] L. Barron, Symmetry and molecular chirality, *Chemical Society Reviews* **15**, 189 (1986).
- [72] J. L. Greenfield, J. Wade, J. R. Brandt, X. Shi, T. J. Penfold, and M. J. Fuchter, Pathways to increase the dissymmetry in the interaction of chiral light and chiral molecules, *Chemical Science* **12**, 8589 (2021).
- [73] Y. Liu and B. Yan, Anomalous circularly polarized light emission induced by the optical berry curvature dipole, *Physical Review B* **109**, 035142 (2024).
- [74] X. Shang, L. Wan, L. Wang, F. Gao, and H. Li, Emerging materials for circularly polarized light detection, *Journal of Materials Chemistry C* **10**, 2400 (2022).
- [75] A. Nitzan, *Chemical dynamics in condensed phases: relaxation, transfer and reactions in condensed molecular systems*

(Oxford university press, 2006).

- [76] J. P. Malhado and J. T. Hynes, Photoisomerization for a model protonated schiff base in solution: Sloped/peaked conical intersection perspective, *The Journal of Chemical Physics* **137**, 22A543 (2012).
- [77] V. Mosallanejad, J. Chen, and W. Dou, Floquet-driven frictional effects, *Physical Review B* **107**, 184314 (2023).
- [78] J. Chen, W. Liu, and W. Dou, Floquet nonadiabatic nuclear dynamics with photoinduced lorenz-like force in quantum transport, arXiv preprint arXiv:2308.12660 (2023).
- [79] H. Haug, A.-P. Jauho, *et al.*, *Quantum kinetics in transport and optics of semiconductors*, Vol. 2 (Springer, 2008).
- [80] Y. Meir and N. S. Wingreen, Landauer formula for the current through an interacting electron region, *Physical review letters* **68**, 2512 (1992).
- [81] N. Bode, S. V. Kusminskiy, R. Egger, and F. Von Oppen, Scattering theory of current-induced forces in mesoscopic systems, *Physical review letters* **107**, 036804 (2011).